Unconditionally-Stable Meshless Methods Using Different Split-Step Techniques and Their Phase Velocity Considerations

F. Ansarizadeh [1] and M. Movahhedi [2]

[1] Department of Electrical Engineering,
Shahid Bahonar University of Kerman, Kerman, Iran
f.ansarizadeh@eng.uk.ac.ir

[2] Department of Electrical and Computer Engineering,
Yazd University, Yazd, Iran
movahhedi@ieee.org

Abstract ─ In this paper, new unconditionally-stable meshless methods based on different split-step methods are proposed. Moreover, comparison of the phase velocities of two different split-step meshless methods and that of alternative-direction-implicit meshless (ADI-ML) method is presented. Here we show how employing split-step (SS) technique using radial point interpolation meshless (RPIM) method results in an unconditionally stable scheme. Symmetric operators and uniform splitting are utilized simultaneously to split the classical Maxwell's matrix into four and six submatrices. Also, for more accurate approximations Crank-Nicolson (CN) scheme that is a fully implicit scheme has been applied for implementation of these schemes. It has been demonstrated, these proposed methods produce even more effective unconditionally stable responses than those of alternating-direction-implicit meshless time-domain ADI-MLTD methods. Eventually, in order to prove the advantage of the proposed method, a comparison has been made between these novel meshless methods and their finite-difference counterparts. More smoothed phase velocities in proposed meshless methods imply a reduction in dispersion error in comparison with their analogous cases in finite-difference time-domain (FDTD) method.

Index Terms - Meshless methods, phase velocity, radial basis function (RBF), split-step (SS), and unconditionally stable.

I. INTRODUCTION

Over two recent decades special attention has been allocated to solve Maxwell's curl equations in time-domain. The main reason can be attributed to the unique capability of time-domain in solving ultra wide band (UWB) problems in only a single run and also modeling medium, which possesses nonlinear properties or/and consists of different materials and consequently different permittivity coefficients. Unfortunately, if the geometry of the problem domain is too complicated, demanding high resolution, dependency of time step size on the smallest space step leads in a time-consuming simulation process that is undesirable [1].

Meshless methods have newly been proved to be appropriate alternatives to the finite-element (FE) methods, due to their property of avoiding meshing and remeshing, in addition to the capability of effective treatment of complicated geometries [2]. Using meshless methods, it is simply possible to locate more nodes in the regions that have fast variations of fields and this way capture these variations to ameliorate the accuracy. On the other hand, in the regions fields have slow changes fewer nodes can be located that is so economical in aspects of CPU usage time and the memory needed [3]. Amidst the diverse meshless methods, the radial basis function (RBF), which brought forward by Kansa [4] in 1990, is the most prevailing technique in solving partial differential equations (PDEs) due to its accuracy, consistency and ease of implementation [5]. Applying RBF in meshless methods, unknown

functions of PDEs or integral equations are interpolated at the scattered nodes and point matching method is applied to the equation at the collocation nodes [6].

As mentioned before, choosing small time-step size leads in a time-consuming simulation process that is not desirable. The possibility of choosing larger time-step size helps to reduce the computational and simulation time, that is why searching for unconditionally stable schemes that permit several order larger time step size have been the aim of many studies and researches lately. Using meshless methods to solve time domain electromagnetic problems with large time steps, acquire advantages of both meshless and unconditionally stable methods simultaneously. Recently an unconditionally stable method based on leapfrog alternating-direction-implicit scheme using radial point interpolation meshless (RPIM) method in three-dimensional (3-D) has been presented in [7] that outperforms the LOD-RPIM method in terms of computational effort [8]. In 2011, a new unconditionally stable scheme based on (RPIM) method using the weighted Laguerre polynomials has been introduced in [3]. Through this technique, which is marching-on-in-degree method instead of marching-on-in-time one, the time step is used only to calculate the Laguerre expansion coefficients of sources done only at the start of the computations. Thus, the stability is not affected by the time step size any more.

Here, the split-step scheme, which divides a complete time step into several identical sub steps, for example 6 sub steps (6 SS), has been chosen to reach an unconditionally stable meshless method. Using uniform splitting operators in a special way, which explained later, 6 SS and 4 SS have the same formulations but different coefficients. To clarify the proposed technique, 6 SS-MLTD discussed in details and the same goes for 4 SS-MLTD scheme.

II. CONSTRUCTION OF SPLIT-STEP TECHNIQUE

Dealing with 6 SS-MLTD, for each time step we need only to advance six one-dimensional (1-D) equations, permitting high computational speed together with unconditional stability. Here for simplicity a TE$_z$ wave is considered in order to implement the proposed method. It is completely clear that this simplification does not affect the generality of the method adversely.

A. Split step technique

According to the explained situation Maxwell's equations can be written down in matrix form as,

$$\frac{\partial \vec{u}}{\partial t} = \mathbf{M}\,\vec{u}. \tag{1}$$

where the fields' vector and Maxwell's matrix has considered as,

$$\vec{u} = \left(E_x, E_y, H_z\right)^{\mathrm{T}}. \tag{2}$$

$$\mathbf{M} = \begin{bmatrix} 0 & 0 & \dfrac{\partial}{\varepsilon\partial y} \\ 0 & 0 & -\dfrac{\partial}{\varepsilon\partial x} \\ \dfrac{\partial}{\mu\partial y} & -\dfrac{\partial}{\mu\partial x} & 0 \end{bmatrix}. \tag{3}$$

while μ and ε are the permeability and permittivity of the medium, respectively. As mentioned before, here 6 SS-MLTD method is explained completely and 4 SS-MLTD method can be inferred from this procedure.

B. The split-step meshless methods

At first, symmetric operator and uniform splitting technique are applied to disintegrate the matrix M into six components while matrix A$_x$ and matrix A$_y$ illustrate spatial derivatives in the x- and y-directions, respectively

$$\mathbf{A}_x = \begin{bmatrix} 0 & 0 & 0 \\ 0 & 0 & -\dfrac{\partial}{\varepsilon\partial x} \\ 0 & -\dfrac{\partial}{\mu\partial x} & 0 \end{bmatrix}, \tag{4-a}$$

$$\mathbf{A}_y = \begin{bmatrix} 0 & 0 & \dfrac{\partial}{\varepsilon\partial y} \\ 0 & 0 & 0 \\ \dfrac{\partial}{\mu\partial y} & 0 & 0 \end{bmatrix}. \tag{4-b}$$

Exploiting the split-step technique, in this work we consider this permutation for these six sub-matrices,

$$\mathbf{M} = \left(\frac{\mathbf{A}_x}{3}\right) + \left(\frac{\mathbf{A}_y}{3}\right) + \left(\frac{\mathbf{A}_x}{3}\right)$$
$$+ \tag{5}$$
$$\left(\frac{\mathbf{A}_y}{3}\right) + \left(\frac{\mathbf{A}_x}{3}\right) + \left(\frac{\mathbf{A}_y}{3}\right).$$

Here it is worth mentioning that there is possibility of leading to unconditionally stable schemes for other permutations of these sub-

matrices just like the FDTD counterparts of this technique [9]. Hence, the time step size is divided into six identical sub-steps. These sub-steps produce some intermediate solution that are nonphysical and just help to reach more accurate results [4]. At the bottom, two of these equations present successive odd and even sub-steps, respectively,

$$\frac{\partial \vec{u}}{\partial t} = 6.\left(\frac{\mathbf{A}_x}{3}\right)\vec{u}, \quad t \to t + 1/6. \qquad (6\text{-}a)$$

$$\frac{\partial \vec{u}}{\partial t} = 6.\left(\frac{\mathbf{A}_y}{3}\right)\vec{u}, \qquad t + 1/6 \to t + 2/6. \qquad (6\text{-}b)$$

As time marches these equations repeat for odd and even time sub-steps.

Here in right hand side (RHS) of the equations we use Crank-Nicolson (CN) scheme, which is unconditionally stable for more accurate results [10]. In this scheme spatial derivatives replace with the average value of two adjacent moments of the spatial derivatives. This way we get these equations for two odd and even successive sub-steps, respectively

$$\left([\mathbf{I}] - \frac{\Delta t}{6}\mathbf{A}_x\right)\vec{u}^{t+1/6} = \left([\mathbf{I}] + \frac{\Delta t}{6}\mathbf{A}_x\right)\vec{u}^t, \qquad (7\text{-}a)$$

$$\left([\mathbf{I}] - \frac{\Delta t}{6}\mathbf{A}_y\right)\vec{u}^{t+2/6} = \left([\mathbf{I}] + \frac{\Delta t}{6}\mathbf{A}_y\right)\vec{u}^{t+1/6}. \qquad (7\text{-}b)$$

Now in the next stage these equations are expressed in meshless method. Before implementation of these formulations in meshless method there is a brief explanation about this technique.

III. THE CONVENTIONAL RPIM METHOD

A. Equation formatting

Here Maxwell's equations have been discretized through RBF method. In RPIM methods the value of the field variable u(x) is interpolated using the value of the field nodes those are enclosed by the encompassing of the support domain of arbitrary point x, as described in [2]. If we assume $x = (x,y)^T$ to be the arbitrary point at which u(x) is to be approximated, desired unknown can be achieved using the following equation,

$$u(\mathbf{x}) = \sum_{i=1}^{n} r_n(\mathbf{x})\, a_n + \sum_{j=1}^{m} p_m(\mathbf{x})\, b_m. \qquad (8)$$

while n is the number of nodes surrounded by the support domain of arbitrary point $x=(x,y)^T$, $r_n(x)$ is the radial basis function, p_m (x) is the monomial basis function, a_n and b_m are coefficients yet to be determined. Since its derivatives are different from the original function only in a constant coefficient and thus more efficient in mathematical handling, the Gaussian function is selected as the radial basis function,

$$r_n(\mathbf{x}) = exp\left(-c\left|\frac{r}{r_{max}}\right|^2\right). \qquad (9)$$

$$r = \sqrt{\left(x - x_j\right)^2 + \left(y - y_j\right)^2}. \qquad (10)$$

where r_{max} and (x_i, y_i) describe the diameter of the support domain corresponding to the arbitrary point x, and location of ith node within it, respectively. Here c represents the shape parameter of the Gaussian radial basis function that controls the decaying rate of the function.

B. Choosing shape parameters

Shape parameters are so influential in basis functions and consequently the results of supposed electromagnetic problem that they also called control parameters. Basically, seeking the best shape parameters maintaining a good balance between accuracy and stability, relies on trial and error that is a costly and time consuming process. In reality, the freedom to choose shape parameters is not a positive point [11]. Up to now, there has not any calculable way to find the best shape parameters, easily, and thus choosing the optimal shape parameters is an attractive research area. In this paper r_{max} chooses equal to the size of space step (ΔS) and another shape parameter, i.e., c, finds by trial and error to give the best practical results in accordance with the electromagnetic fields propagation in the time domain and desired cut-off frequency.

IV. NUMERICAL EXPERIMENT AND DISCUSSION

As mentioned, we consider a TE_z 2-D wave propagating in a homogeneous, linear, isotropic and lossless medium. Here a 1 *cm* × 1 *cm* cavity filled with air and terminated with perfect electric conductor (PEC) boundaries has been selected in the *x-y* plane. Thus, in order to have symmetric

excitation, a magnetic current density in the form of modulated Gaussian pulse function has been exploited as,

$$\mathbf{M}_{sz} = \mathbf{M}_0 exp\left(-\left(\frac{t-t_0}{\tau}\right)^2\right) * \\ sin(2\pi f(t-t_0)). \tag{11}$$

For simplicity it is supposed that $a = \Delta t/6\varepsilon$ and b = $\Delta t/6\mu$. With the definition of E-nodes and H-nodes at the same location and using the central difference scheme to approximate the time derivatives, the field variables in Maxwell's curl equations can be approximated as follows:

For the first sub-step,

$$E_{x,i}^{t+1/6} = E_{x,i}^t, \tag{12-a}$$

$$E_{y,i}^{t+1/6} = E_{y,i}^t - a \\ \times\left(\sum_j \partial x \Phi_j H_{z,j}^t + \sum_j \partial x \Phi_j H_{z,j}^{t+1/6}\right), \tag{12-b}$$

$$H_{z,i}^{t+1/6} = H_{z,i}^t - b \\ \times\left(\sum_j \partial x \Phi_j E_{y,j}^t + \sum_j \partial x \Phi_j E_{y,j}^{t+1/6}\right). \tag{12-c}$$

For the second sub-step,

$$E_{x,i}^{t+2/6} = E_{x,i}^{t+1/6} + a \\ \times\left(\sum_j \partial y \Phi_j H_{z,j}^{t+1/6} + \sum_j \partial y \Phi_j H_{z,j}^{t+2/6}\right), \tag{12-d}$$

$$E_{y,i}^{t+2/6} = E_{y,i}^{t+1/6}, \tag{12-e}$$

$$H_{z,i}^{t+2/6} = H_{z,i}^{t+1/6} + b \\ \times\left(\sum_j \partial y \Phi_j E_{x,j}^{t+1/6} + \sum_j \partial y \Phi_j E_{x,j}^{t+2/6}\right). \tag{12-f}$$

It is completely clear that other odd and even sub-steps have the same formulations, but different time intervals. Namely, this procedure repeats for the other four remaining sub-steps, respectively. This way the other update equations can be attained analogously. It is worth mentioning that in all simulated schemes, space step size is selected $\Delta S = 0.5$ mm. According to the dimensions of the supposed cavity, there are 21×21 nodes under scrutiny. Based on intrinsic difference between meshless and finite-difference methods under stipulated conditions, there are 20×20 cells in finite-difference methods. Number of unknowns in all FD-TD and ML-TD methods is equal to the number of cells and nodes, respectively. The subtle point here that is worth pondering is multiplying time sub-steps in ADI-MLTD, 4SS-MLTD, and 6SS-MLTD methods by 2, 4, and 6, respectively. Field values at these sub-steps leads to intermediate solutions those have no physical meaning and just used to update the field value variations for the next sub-steps. To analyze the assumed problem, the current source excites the cavity at its center.

Tables 1, 2, and 3 show the simulation results of the cavity analysis for its dominant mode cut-off frequency. Acceptable variations of cut-off frequency and also stability of the electromagnetic field in time-domain by increasing time step size reveal that split-step meshless time-domain methods (4SS-MLTD and 6SS-MLTD methods) are unconditionally stable. Moreover in general, 6SS-MLTD method shows more accurate results for cut-off frequencies while increasing the time step size in comparison with 4SS-MLTD method and even ADI-MLTD method.

Table 1: Simulation results of cavity analysis for its dominant mode cut-off frequency and CPU time by ADI-MLTD method.

Time-step size	Time sub-steps number	Cut-off frequency TE_{z10} (GHz)	Relative error (%)	CPU time (sec)
τ	4730	15.421	2.806	251.1642
2τ	2365	15.642	4.280	129.6259
4τ	1183	15.834	5.560	68.2512
6τ	788	15.124	0.827	48.076
8τ	591	15.476	3.173	37.746

Table 2: Simulation results of cavity analysis for its dominant mode cut-off frequency and CPU time by SS4-MLTD.

Time-step size	Time sub-steps number	Cut-off frequency TE_{z10} (GHz)	Relative error (%)	CPU time (sec)
τ	9461	15.156	1.04	102.435
2τ	4730	15.184	1.227	55.066
4τ	2365	15.145	0.967	31.270
6τ	1577	15.265	1.767	23.004
8τ	1183	15.462	3.08	19.016

Table 3: Simulation results of cavity analysis for its dominant mode cut-off frequency and CPU time by SS6-MLTD.

Time-step size	Time sub-steps number	Cut-off frequency TE_{z10} (GHz)	Relative error (%)	CPU time (sec)
τ	14191	15.141	0.94	591.410
2τ	7096	15. 162	1.08	411.996
4τ	3547	15.158	1.053	288.447
6τ	2365	15.214	1.427	102.463
8τ	1773	15.248	1.653	79.488

In this paper, variation of phase velocity in different directions, which is considered as the main source of dispersion error is disserted. Phase velocity can be found via $v_p = \Delta S/\Delta t$, while ΔS is the displacement of an arbitrary point with a specific phase of propagating wave in the time interval Δt. Considering the speed of electromagnetic waves in vacuum, i.e., $c = 3 \times 10^8$, as the criterion of measurement, the phase velocities in all directions are normalized dividing by this specific velocity. In other words, it can be indicated as normalized phase velocities = v_p/c.

Speaking of FDTD method, the Yee space lattice represents an anisotropic medium because in such lattice, propagation velocity is dependent on the direction of wave propagation, which causes different phase velocities in different angles of propagation. In more detailed words, the phase velocity has its maximum along the grid diagonals and its minimum along the major axis of the grid. Anisotropic phase velocity plays a key role in dispersion errors [12].

Against FDTD methods, there is not any closed form formula to calculate phase velocity in meshless methods. Facing meshless methods, phase velocity in different directions must be calculated through tracing the electromagnetic wave before reflecting back from the boundaries in different time intervals in different angles of propagation. This process can be done easily for specific angels like φ = 0º, 45º, 90º, 135º, and 180º. For other angels using more dense nodes it is possible to calculate phase velocities in other angels. Putting these phase velocities together and using interpolation, the following curves are deduced.

Figure 1 illustrates the normalized phase velocities of different split step schemes for meshless and finite-difference time-domain methods versus wave propagation angles. Here PPW stands for "point per wavelength" that is PPW = λ/ΔS, where λ stands for wavelength. PPW has similar meaning to cell per wavelength (CPW) in finite-difference method. Moreover, Fig. 2 shows the phase velocity of ADI-MLTD and ADI-FDTD methods as a function of propagation direction. Based on Figs. 1 and 2, numerical experiments reveal this fact that using meshless methods there is not such a great difference between phase velocities in different directions. In other words, comparing these results with their counterparts in FDTD method [13] it can be concluded that modeling geometry with nodes not cells namely meshless methods instead of finite-difference methods, results in more smoothed phase velocities in different directions and consequently lower dispersion errors. It is resulted from changing shape parameters, the least dispersion error is related to optimal shape parameters and any variations in shape parameters aggrandizes dispersion errors. More investigations endorse this result for any rectangular cavity. In sense of velocity, it is completely clear that 6SS-MLTD method outperforms 4SS-MLTD method and the same goes for 4SS4-MLTD proportional to ADI-MLTD methods.
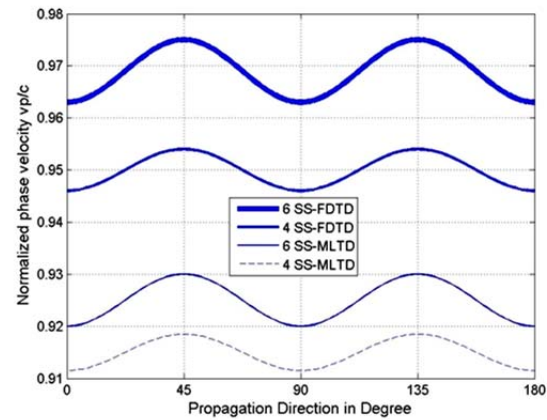

Fig. 1. Normalized phase velocities as a function of propagation angle for PPW = 41.

In these curves the smoother propagation in different directions, the less dispersion error there is in the scheme. Just like what occurred in FDTD method on examination of the phase velocity [10], ADI-MLTD method have worse anisotropy phase velocity than that of the four and six split-step

meshless methods. It means ADI-MLTD method has much larger anisotropy error in comparison with split-step methods. This fact guarantees better function of SS-MLTD methods than ADI-MLTD method. Here, all simulations are performed on an Intel Corei7 CPU with 4 GB RAM and 1.73 GHz. Memory usage in 6SS-MLTD methods is about 51% while in 4SS-MLTD and ADI-MLTD methods this factor decreases to 48%. Since the processor has to deal with more equations, it seems to be logical using higher memory in 6SS-MLTD.
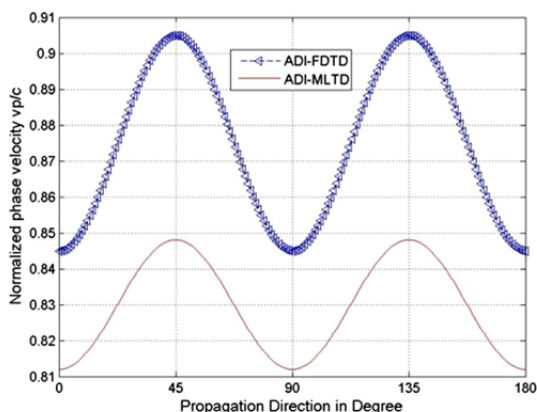

Fig. 2. Comparison between normalized phase velocities of ADI-MLTD (PPW = 40) and ADI-FDTD.

V. CONCLUSIONS

Two different split-step meshless time-domain (SS-MLTD) methods have been proposed in this paper. 4SS-MLTD and 6SS-MLTD techniques perform by splitting the Maxwell's matrix into four and six sub-matrices and simultaneously dividing the time-step into four and six equal sub-steps, respectively. These schemes brought up in this paper reduce the anisotropy of phase velocity in different directions of propagation. In other words, normalized phase velocities in SS-MLTD methods is smoother than what it is in ADI-MLTD method and as a consequence this proposed scheme lead in lower dispersion error. Additionally, it was observed just like what occurred in FDTD method, 4SS-MLTD shows more smoothed changes in different direction in respect with 6SS-MLTD method and thus less adverse dispersion errors. This will lead to useful unconditionally stable meshless methods with low dispersion error.

REFERENCES

[1] R. Mirzavand and A. Abdipour, "Unconditionally stable MFLTD method for the full-wave electromagnetic simulation," *IEEE Trans. Antennas Propagat.*, vol. 60, no. 5, May 2012.

[2] G. Liu and G. Gu, *An Introduction to Meshfree Methods and Their Programming*, Springer 2005.

[3] X. Chen, Z. Chen, Y. Yu, and D. Su, "An unconditionally stable radial point interpolation meshless method with Laguerre polynomials," *IEEE Trans. Antennas Propagat.*, vol. 59, no. 10, Oct. 2011.

[4] E. Kansa, "Multiqudrics—A scattered data approximation scheme with applications to computational fluid-dynamics—I. Surface approximations and partial derivatives," *Appl. Comput. Math.*, vol. 19, no. 8–9, pp. 127-145, Sept. 1992.

[5] Y. Yu, F. Jolani, and Z. (David) Chen, "An efficient meshless approach to multi-scale modeling in the time-domain," *Applied Computational Electromagnetic Society (ACES) Journal*, vol. 27, no. 6, June 2012.

[6] S. Lai, B. Wang, and Y. Duan, "Meshless radial basis functions method for solving Hallen's Integral equation," *Applied Computational Electromagnetic Society (ACES) Journal*, vol. 27, no. 1, Jan. 2012.

[7] Y. Yu and Z. Chen, "Towards the development of an unconditionally stable time-domain meshless method," *IEEE Trans. Microw. Theory Tech.,* vol. 58, no. 3, pp. 578-586, March 2010.

[8] Y. Yu and Z. Chen, "Towards the development of unconditionally stable time-domain meshless numerical methods," in *IEEE MTT-S Int. Microw. Symp. Dig.,* Boston, MA, pp. 309-312, 7-12 June 2009.

[9] Q. Chu and Y. Kong, "Three new unconditionally-stable FDTD methods with high-order accuracy," *IEEE Trans. Antennas Propagat.,* vol. 57, no. 9, Sept. 2009.

[10] G. Sun and C. Trueman, "Unconditionally stable Crank-Nicolson scheme for solving two-dimensional Maxwell's equations," *Electronics Lett.,* 3rd vol. 39, no. 7, April 2003.

[11] G. Fasshuar and J. Zhang, "On choosing optimal shape parameters for RBF approximation," *Mathematics Subject Classification* 65D05. 65D15.65M70, 2000.

[12] A. Taflove and S. Hangess, *Computational Electrodynamtics: The Finite-Difference Time-Domain Method*, Boston, MA: Artech House, 2005.

[13] M. Kusaf and A. Oztoprak, "An unconditionally stable split-step FDTD method for low anisotropy,"

IEEE Microwave and Wireless Compo. Lett., vol. 18, no. 4, pp. 224-226, April 2008.

Fatimah Ansarizadeh received the B.Sc. and M.Sc. in Electrical Engineering from Shahid Bahonar University of Kerman, Kerman, Iran in 2007 and 2013. Her current research interest is using Meshmfree methods to solving electromagnetic problems.
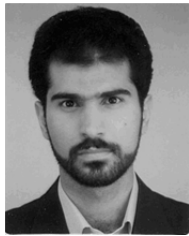
Masoud Movahhedi was born in Yazd, Iran, in 1976. He received the B.Sc. degree from Sharif University of Technology, Tehran, Iran, in 1998, the M.Sc. degree from Amirkabir University of Technology (Tehran Polytechnic), Tehran, Iran, in 2000, both in Electrical Engineering, and also Ph.D. degree in Electrical Engineering at the same University in 2006. In December 2005, he joined the Institute for Microelectronics, Vienna University of Technology, Vienna, Austria, as a Visiting Student and now is an Assistant Professor in Electrical and Computer Engineering Department at Yazd University. His research interests are in the areas of computer-aided design of microwave integrated circuits, computational electromagnetic, semiconductor high-frequency RF modeling, and metamaterials.

Dr. Movahhedi was the recipient of the GAAS-05 Fellowship sponsored by the GAAS Association to young graduate researchers for his paper presented at GAAS2005. He was also the recipient of the Electrical Engineering Department outstanding student award in 2006.